

1 **Title: Immune response to the mRNA COVID-19 vaccine in hemodialysis patients: cohort study**

2 **Authors:** Yi-Shin Chang^{1,2*}, Kai Huang^{1,2*}, Jessica M Lee^{1,3}, Christen L Vagts¹, Christian Ascoli¹, Md-Ruhul
3 Amin¹, Mahmood Ghassemi¹, Claudia M Lora¹, Russell Edafetanure-Ibeh¹, Yue Huang¹, Ruth A Cherian¹,
4 Nandini Sarup¹, Samantha R Warpecha¹, Sunghyun Hwang¹, Rhea Goel¹, Benjamin A Turturice^{1,3,4}, Cody
5 Schott^{1,3,5}, Montserrat Hernandez¹, Yang Chen^{1,6}, Julianne Joregensen^{1,2}, Wangfei Wang^{1,2}, Mladen
6 Rasic^{1,2}, Richard M Novak¹, Patricia W Finn^{1,2,3**}, David L Perkins^{1,2,6**}

7 **Affiliations:**

- 8 1. Department of Medicine, University of Illinois at Chicago, Chicago, Illinois, USA
9 2. Department of Bioengineering, University of Illinois at Chicago, Chicago, Illinois, USA
10 3. Department of Microbiology and Immunology, University of Illinois at Chicago, Chicago, Illinois,
11 USA
12 4. Department of Medicine, Stanford University, Palo Alto, California, USA
13 5. Department of Medicine, University of Colorado Denver, Aurora, Colorado, USA
14 6. Department of Biological Sciences, University of Illinois at Chicago, Chicago, Illinois, USA

15 *These authors contributed equally.

16 **These authors contributed equally.

17

18

19

20

21

22

23 **Corresponding author:**

24 Patricia W. Finn, MD

25 840 S. Wood St.

26 CSB 1020N, MC 787

27 Chicago, IL 60612

28 312-413-1279

29 pwfinn@uic.edu

30

31 **Funding:** F30HD102093, F30HL151182, T32HL144909, R01HL138628

32 This research has been funded by the University of Illinois at Chicago Center for Clinical and

33 Translational Science (CCTS) award UL1TR002003

34

35 **Keywords:** RNA Sequencing, COVID-19, Vaccine, SARS-CoV-2, Hemodialysis, binding antibodies,

36 neutralizing antibodies

37

38

39

40 **Abstract**

41 **Background:** End-stage renal disease (ESRD) patients experience immune compromise characterized by
42 complex alterations of both innate and adaptive immunity, and results in higher susceptibility to
43 infection and lower response to vaccination. This immune compromise, coupled with greater risk of
44 exposure to infectious disease at hemodialysis (HD) centers, underscores the need for examination of
45 the immune response to the COVID-19 mRNA-based vaccines.

46 **Methods:** A transcriptomic analysis of the immune response to the Covid-19 BNT162b2 mRNA vaccine
47 was assessed in 20 HD patients and cohort-matched controls. RNA sequencing of peripheral blood
48 mononuclear cells (PBMCs) was performed longitudinally before and after each vaccination dose for a
49 total of six time points per subject. Anti-spike antibody levels were quantified prior to the first
50 vaccination dose (V1D0) and seven days after the second dose (V2D7) using anti-Spike IgG titers and
51 antibody neutralization assays. Anti-spike IgG titers were additionally quantified six months after initial
52 vaccination. Clinical history and lab values in HD patients were obtained to identify predictors of
53 vaccination response.

54 **Results:** Transcriptomic analyses demonstrated differing time courses of immune responses, with
55 predominant T cell activity in controls one week after the first vaccination dose, compared to
56 predominant myeloid cell activity in HD at this time point. HD demonstrated decreased metabolic
57 activity and decreased antigen presentation compared to controls after the second vaccination dose.
58 Anti-spike IgG titers and neutralizing function were substantially elevated in both controls and HD at
59 V2D7, with a small but significant reduction in titers in HD groups ($p < 0.05$). Anti-spike IgG remained
60 elevated above baseline at six months in both subject groups. Anti-spike IgG titers at V2D7 were highly
61 predictive of 6-month titer levels. Transcriptomic biomarkers after the second vaccination dose and
62 clinical biomarkers including ferritin levels were found to be predictive of antibody development.

63 **Conclusion:** Overall, we demonstrate differing time courses of immune responses to the BNT162b2
64 mRNA COVID-19 vaccination in maintenance hemodialysis subjects (HD) comparable to healthy controls
65 (HC) and identify transcriptomic and clinical predictors of anti-Spike IgG titers in HD. Analyzing
66 vaccination as an in vivo perturbation, our results warrant further characterization of the immune
67 dysregulation of end stage renal disease (ESRD).

68 **Funding:** F30HD102093, F30HL151182, T32HL144909, R01HL138628

69 This research has been funded by the University of Illinois at Chicago Center for Clinical and

70 Translational Science (CCTS) award UL1TR002003

71

72

73

74 **Background:**

75 End-stage renal disease (ESRD) is the most advanced stage of chronic kidney disease (CKD), with
76 prevalence in the U.S. reaching 809,000 in 2019 ¹. The most used form of renal replacement therapy for
77 ESRD patients in the U.S. is hemodialysis (HD). Despite significant improvements in hemodialysis
78 technology, the mortality rate in ESRD patients is still as high as 20% annually ², with infections being the
79 most common cause of hospitalization and mortality after cardiovascular disease ³. The
80 immunocompromised state of ESRD is characterized by simultaneous immunodepression due to the
81 impact of uremic milieu on immunocompetent cells and immunoactivation due to the accumulation of
82 proinflammatory cytokines ³. There are alterations to both innate and adaptive immunity, including
83 elevated levels of mannose-binding lectin ⁴, impaired maturation of monocytes and dendritic cells ^{4,5},
84 increased B cell apoptosis ⁶, and decreased T-cell proliferation with elevated Th1/Th2 ratio⁷.

85

86 Studies of genome-wide expression (i.e. transcriptome) profiles of peripheral blood mononuclear cells in
87 ESRD demonstrate a complex picture of immune alterations. One study found upregulation of genes
88 involved in the complement and oxidative metabolism pathways, and downregulation of genes
89 associated with the clathrin-coated vesicle endosomal pathway and T-cell receptor signaling ¹⁰. Two
90 other studies have demonstrated impaired expression of genes involved in oxidative phosphorylation
91 and mitochondrial function ^{11,12}. A study identifying a group of inflammatory genes playing a causative
92 role in oxidative stress in dialysis patients showed unique gene expression alterations in maintenance
93 HD patients compared to un-dialyzed CKD patients and compared to patients undergoing peritoneal
94 dialysis ¹³. These studies indicate a range of immune pathways that may impair vaccination response,
95 and further suggest that dialysis leads to unique immune profile alterations. These alterations may lead
96 to higher susceptibility to infection and lower response to vaccination ⁸. For example, while more than

97 90% of patients without CKD develop protective antibodies against HBV after vaccination, only 50-60%
98 of patients with ESRD seroconvert. There have also been higher vaccination failure rates demonstrated
99 against influenza virus, Clostridium tetani, and Corynebacterium diphtheriae in ESRD⁹.

100

101 Understanding the immune response to vaccines in ESRD is particularly important for the new mRNA
102 vaccines developed in response to the COVID-19 pandemic. The COVID-19 mRNA-based vaccines,
103 BNT162b2 and mRNA-1273, have proven to be efficacious in non-immunocompromised individuals, with
104 initial reports showing 95% and 94.1% reduction of COVID-19 disease in recipients^{14,15}. However, certain
105 immunosuppressed populations remain at risk of infection. Given the widespread transmission of
106 COVID-19, detailed assessments of degree, duration, and determinants of immune protection conferred
107 by these vaccines are vitally needed in immunocompromised patient populations including those with
108 ESRD.

109

110 While recent studies of the SARS-CoV-2 BNT162b2 vaccine in HD demonstrate high levels of
111 seroconversion ranging from 84-96%¹⁶⁻¹⁹, they also demonstrate quantitatively reduced SARS-CoV-2 IgG
112 antibodies. We posit that characterization of the transcriptomic underpinnings of antibody titer
113 development on a continuous scale may identify biomarkers for weaker or less durable immune
114 protection in this population. Furthermore, transcriptomic analyses may identify strategies for the
115 development of new, effective vaccines against other infectious diseases for this population. Thus, we
116 characterized the immune response of the HD population to the COVID-19 mRNA-based BNT162b2
117 vaccine using mRNA sequencing, anti-spike antibody ELISA and neutralization titers across multiple time
118 points. We then integrated these data to identify transcriptomic and clinical determinants of the
119 humoral immune response in HD patients.

120

121 **Methods:**

122 *Study population and sample acquisition*

123 The study was approved by the University of Illinois at Chicago IRB (#2018-1038) Ethics Review
124 Committee. Maintenance HD patients undergoing vaccination with the BNT162b2 mRNA COVID-19
125 vaccine in February 2021 were recruited from the outpatient HD unit at the University of Illinois Hospital
126 (UIH) in Chicago, IL. Control subjects consisted of UIH employees undergoing BNT162b2 mRNA COVID-19
127 vaccination at UIH from December 2020 to January 2021 with no self-reported history of kidney disease
128 or immune disorders. A subset of control subjects matched for age, gender, and COVID-19 history was
129 also analyzed for this study. Blood was collected at 0 – 48 hours prior to and at multiple time points
130 after both the first (V1) and second vaccination doses (V2), which were administered three weeks apart.
131 Control samples were collected prior to each vaccination dose (D0) and at one day (D1) and seven days
132 (D7) after each dose, corresponding to six time points: V1D0, V1D1, V1D7, V2D0, V2D1, V2D7. Blood was
133 collected from HD subjects prior to each vaccination dose and at two days (D2) and seven days after
134 each dose, corresponding to six time points: V1D0, V1D2, V1D7, V2D0, V2D2, V2D7. A final blood sample
135 was drawn six months after initial vaccination (M6) for measurement of antibody titers, prior to
136 additional vaccination doses. Serum and peripheral blood mononuclear cells (PBMCs) were extracted
137 within two hours of blood collection, then stored at -80°C. PBMCs were extracted using density gradient
138 centrifugation at 400g with Ficoll-Paque PLUS. The extracted buffy coat was stored in RNAlater
139 (Invitrogen).

140 *Clinical and Demographic Characterization*

141 Demographic and clinical data was collected from the electronic health record (EHR) for HD subjects,
142 including medical diagnoses, medications, and laboratory values. Laboratory values included monthly
143 SARS-CoV-2 test results, as well as urea reduction ratio (URR, a measure of dialysis adequacy),
144 hemoglobin (Hgb), ferritin, transferrin saturation, albumin levels, white blood cell (WBC) count and WBC

145 differential counts obtained during standard of care monthly blood draws for the three months
146 preceding vaccination. Within our analyses, ferritin was coded as either low risk (200ng/ml – 1200
147 ng/ml) or high risk (<200 ng/ml or >1200 ng/ml), since ferritin levels 200ng/ml – 1200 ng/ml have been
148 shown to be associated with lowest all-cause mortality in HD patients²⁰. Baseline clinical lab values were
149 calculated as the median of three lab values across the three months prior to vaccination. Demographic
150 and clinical data was collected from a medical questionnaire at time of consent for control subjects, and
151 included medical history, medications, and self-reported prior SARS-CoV-2 positive test results.

152 *RNA extraction and RNA Sequencing (RNAseq)*

153 RNA sequencing was performed on PBMCs at all V1 and V2 time points for all subjects for whom RNA
154 libraries were successfully built at ≥ 5 time points. PBMCs stored in RNAlater were thawed and diluted
155 1:1 with 1X phosphate buffered saline. The mixture was then pelleted and RNA was extracted using the
156 PureLink RNA Mini kit (Invitrogen). DNase treatment to remove genomic DNA contamination was
157 performed using either the PureLink DNase kit or DNA-free DNA Removal Kit (Invitrogen). Purified RNA
158 in sterile water was stored at -80°C. Each RNA sample was quantified using the Qubit RNA High
159 Sensitivity kit (Invitrogen) and Bioanalyzer RNA Pico kit (Agilent) with RIN \geq 8.

160 For library construction, 50ng of RNA from each sample was aliquoted in 96 well plates. Libraries were
161 generated using the NEBNext Ultra II Directional RNA Library Prep Kit for Illumina with the optional
162 NEBNext Poly(A) mRNA Magnetic Isolation Module (New England BioLabs). Each individual sample
163 library was barcoded during PCR amplification using unique dual indexed i5 and i7 primers from the
164 NEBNext Multiplex Oligos for Illumina kit. Each sample library was quantified using the Qubit DNA High
165 Sensitivity kit and Bioanalyzer DNA High Sensitivity kit. Samples were then pooled and sequenced using
166 the MiSeq Nano V2 kit (Illumina) to check read proportions between samples. Samples with lower-than-
167 expected percentage of reads detected were supplemented with an additional spike-in of sample library

168 to the main pool. The supplemented pooled library was sequenced again using the MiSeq Nano V2 kit to
169 verify adequate adjustment. The finalized library was sequenced using a NovaSeq S2 flow cell configured
170 for 75bp paired end output.

171 *Differential Gene Expression Analysis*

172 Raw demultiplexed reads were filtered using fastp to remove adapters and short reads ²¹. Trimmed
173 reads were then quantified using the Salmon pipeline with an hg38 reference transcriptome index ²².
174 Quantified data was imported into R using the tximeta package ²³ to convert Salmon quantification and
175 index data to a count matrix. Transcript names were extracted and matched using Entrez IDs with the
176 AnnotationHub package ²³. This finalized count matrix was then imported into a DESeqDataset object
177 and normalized using the variance stabilizing transformation in DESeq2.

178 The *DESeq2* R package was used to identify genes that were differentially expressed at each time point
179 after vaccination for each subject group. Specifically, we implemented a design incorporating group-
180 specific condition effects with individual subjects nested within groups. We performed the classical
181 *Deseq2* workflow of estimation of size factors, estimation of dispersion, and negative binomial GLM
182 fitting for β_i and Wald statistics, increasing the maximum number of iterations for estimation of the
183 negative binomial distribution to 500. We then generated contrasts to obtain differentially expressed
184 genes for controls at V1D1 and V1D7 (compared to V1D0), and at V2D1 and V2D7 (compared to V2D0).
185 Differentially expressed genes for HD were similarly obtained at V1D2 and V1D7 (compared to V1D0),
186 and at V2D2 and V2D7 (compared to V2D0). We also directly compared gene expression between
187 controls and HD at V1D7 and at V2D7. The significance threshold to determine differential expression
188 was FDR-adjusted ($p < 0.05$).

189 *Anti-Spike (trimer) IgG Titer Quantification*

190 The Human SARS-CoV-2 Spike (Trimer) IgG ELISA Kit from Invitrogen was used to quantitate IgG to the

191 SARS-CoV-2 spike protein in serum samples at V1D0, V2D7, and M6 time points. All samples were
192 initially diluted 1:100 (in addition to the 1:10 assay buffer dilution on the 96-well plate) and assayed in
193 duplicate, with two-fold serial dilution of the 150,000 units/mL standard control in duplicate for relative
194 quantification. Absorbance at 450 nm was quantified using a *Spark*[®] multimode microplate reader.
195 Samples that produced signals greater than the upper limit of the standard curve were diluted 1:2000
196 and assayed again. IgG concentration was calculated by fitting four-parameter logistic curves to the
197 standard controls and taking the average concentrations of duplicates.

198 *Antibody Neutralization Assays*

199 Neutralization assays were performed on serum samples from V1D0 and V2D7 using SARS-CoV-2
200 pseudotyped virus (pseudovirus). To produce pseudoviruses, an expression plasmid bearing codon-
201 optimized SARS-CoV-2 full length S plasmid was co-transfected into HEK293T cells using the SARS-CoV-2
202 Spike-pseudotyped lentiviral particle Kit (BEI # R-52948). The cell supernatants were collected 72h after
203 transfection, divided into aliquots and cryopreserved at -80 °C.

204 To titrate the pseudovirus, 5×10^3 293T-ACE2 cells were seeded per well in a 96-well plate in DMEM
205 containing 10% FBS and 1% penicillin streptomycin. Twenty-four hours later, the pseudovirus was
206 diluted 1:10, followed by five-fold serial dilutions for a total of nine dilutions, with each dilution
207 performed in six replicate wells. After incubation at 37 °C and 5% (vol/vol) CO₂ for 72h, the luciferase
208 substrate was added to the 96-well plate for chemiluminescence detection. The 50% tissue culture
209 infectious dose (TCID₅₀) of the pseudovirus was calculated according to the Reed-Muench method in
210 the titration macro template ²⁴.

211 Neutralization activity against SARS-2-CoV was measured in a single-round-of-infection assay with
212 pseudoviruses as previously described ²⁵. 5×10^3 293T-ACE2 cells were seeded per well in a 96-well plate.
213 Twenty-four hours later, serial dilutions of the serum samples were performed, incubated for one hour

214 at 37 °C with ~1000 TCID50/ml of pseudovirus, then added to monolayers of ACE2-overexpressing 293T
215 cells in quadruplicate. The cell control with cells alone and the virus control (VC) with pseudovirus were
216 set up in each plate. The target cells were incubated for 65h-72h at 37 °C and 5% (vol/vol) CO₂. Fifty µL
217 of Bright-Glo, reconstituted following manufacturer’s instructions, was added to each well of the 96-well
218 plate and incubated for five minutes at room temperature. The 96-well plate was read by a 96-well
219 luminescence plate reader (Tecan Genius Pro plate reader)²⁶. Percent neutralization was calculated as
220 $100 * ([\text{Virus-only control}] - [\text{Virus plus serum}]) / [\text{Virus-only control}]$, and neutralizing titer levels are
221 reported as the serum dilution required to achieve 50% neutralization (50% inhibitory dilution [ID₅₀])²⁷.
222 The input dilution of serum was 1:20, thus 20 is the lower limit of quantification.

223 *BTM module enrichment analysis*

224 Gene set enrichment analysis was performed for each contrast generated in the DESeq2 analysis above
225 using blood transcription module (BTMs) gene sets²⁸. BTMs with FDR-adjusted $p < 0.05$ were considered
226 significantly enriched. Enriched BTMs were further characterized using the distribution of Wald statistics
227 of membership genes from DESeq2. To summarize BTM analyses, BTMs were categorized into different
228 families: B cells, cell cycle, dendritic cell/antigen presentation, type I interferon (IFN type I), myeloid
229 activity/inflammation/ T/NK cells, and “others”²⁹. The percentage of BTMs in each BTM family with
230 significant enrichment at each time point was then quantified over time.

231 *Statistical analysis of antibody response*

232 To determine the effect of vaccination on anti-spike IgG titers at V2D7 and M6, Kruskal-Wallis tests were
233 performed separately for HD subjects and controls. For each group, anti-spike IgG titer levels were
234 compared to assess for the significant effect of time (V1D0, V2D7, M6), and Wilcoxon rank sum tests
235 were performed with FDR correction to assess significant differences between each pair of time points
236 (V2D7 vs. V1D0, M6 vs. V1D0, M6 vs. V2D7). To determine the effect of vaccination on antibody

237 neutralization activity (ID50) at V2D7, Wilcoxon rank sum tests were performed for each group to
238 compare V2D7 vs. V1D0.

239 Linear models were constructed to establish the effect of prior SARS-CoV-2 infection and subject group
240 on anti-spike IgG titer development at V2D7 and M6 and neutralization activity at V2D7. Specifically, log-
241 transformed V2D7 anti-spike IgG titers or V2D7 neutralization activity (ID50) were modeled as the
242 dependent variable, with subject group (HD or controls), log-transformed V1D0 anti-spike IgG titers or
243 V1D0 neutralization activity (ID50), gender, age, race, and ethnicity as independent predictors. To
244 determine predictors of anti-spike IgG at six months, a linear model was constructed with the log-
245 transformed M6 anti-spike IgG titers as the dependent variable, and V2D7 anti-spike IgG titers, SARS-
246 CoV-2 history, gender, age, race, and ethnicity as independent predictors.

247 *Identification of BTM and clinical predictors of Ab response in HD*

248 BTM predictors of antibody response in HD were identified by first calculating a representative
249 expression level of each BTM per sample, which we will refer to as the eigengene. Specifically, the first
250 principal component of each BTM was calculated using DESeq2-derived variance-stabilized gene counts
251 from each module's member genes across the HD V1 time points, and then across the HD V2 time
252 points. Signs (positive or negative) were assigned to the eigengenes such that samples with higher
253 expression of member genes in a BTM would be given a positive sign, while those with lower overall
254 gene expression would be given a negative sign. This was accomplished for each BTM by (1) computing
255 the median gene expression level across membership genes in a given BTM for each sample, (2)
256 computing the Pearson correlation between the eigengene of the BTM and the median gene expression
257 level across all samples, and (3) multiplying the eigengene of the BTM by -1 if the correlation was
258 negative.

259 Subsequently, we constructed linear models with log-transformed anti-spike IgG at V2D7 as the
260 dependent variable and change in BTM eigengene expression after vaccination as the independent
261 variable, controlling for SARS-CoV-2 history. Separate models were constructed for each BTM that was
262 enriched at each time point after vaccination in HD (V1D2 vs V1D0, V1D7 vs V1D0, V2D2 vs V2D0, V2D0
263 V2D7). Change in BTM expression was calculated as the BTM eigengene after vaccination minus the
264 BTM eigengene before vaccination. P-values were FDR-adjusted across number of enriched BTMs per
265 time point.

266 Additionally, baseline clinical laboratory values predictive of antibody response in the HD subjects were
267 identified. Linear models were separately constructed using URR, ferritin (high risk vs low risk),
268 transferrin saturation, hemoglobin, and WBC count to predict log-transformed anti-spike IgG at V2D7
269 and M6.

270 Finally, clinical laboratory values responding to vaccination that predicted antibody titer response in the
271 HD subjects were identified. Linear models were separately constructed using log-fold change (LFC) from
272 baseline measurements of ferritin (continuous instead of binarized low- and high-risk), transferrin
273 saturation, and WBC count to predict log-transformed anti-spike IgG titers at V2D7 and M6.

274

275 **Results:**

276 *Demographic and Clinical Characterization*

277 Demographic and clinical data of the 20 maintenance hemodialysis (HD) and controls (HC) are
278 summarized in **Table 1**. The racial distribution differed between cohorts with more Black/African
279 American subjects in the HD cohort. The cohorts were otherwise demographically similar. The subjects
280 within the HD cohort had significantly more comorbidities, most notable of which include type 2

281 diabetes mellitus (T2DM), hypertension (HTN), dyslipidemia, and other cardiovascular conditions. The
 282 most common causes of renal failure were T2DM and HTN, with a minority of cases attributed to
 283 anatomic defects (reflux uropathy) and autoimmune conditions (systemic lupus erythematosus and
 284 idiopathic thrombocytopenic purpura).

285 **Table 1. Demographic and clinical data for maintenance hemodialysis and control subjects.**

	Hemodialysis	Control	P-val
Total # of subjects	20	20	
Gender			
Male	11	10	1.0
Female	9	10	1.0
Age (mean (sd))	54 (12)	54 (13)	0.98
Race/Ethnicity			
Black/African American	10	3	0.041
Asian/Pacific Islander	1	2	1.0
White/Caucasian	2	8	0.067
Hispanic/Latinx	7	6	1.0
Other	0	1	1.0
BMI, kg/m² (mean (sd))	27.8 (5.1)	28.7 (6.4)	0.61
Medical History			
Diabetes	11	1	0.0012
Hypertension	18	4	< 0.001
Other CV disease*	9	0	0.0012
Dyslipidemia	10	0	< 0.001
Autoimmune disease**	3	0	0.23
Immunosuppression***	1	0	1.0
Active Malignancy****	1	0	1.0
Positive COVID-19 History	8	5	0.5

286 * Includes coronary artery disease (CAD), congestive heart failure (CHF), atrial fibrillation (AF), peripheral
 287 vascular disease (PVD), and cerebral vascular accident (CVA)

288 ** includes systemic lupus erythematosus (SLE), immune thrombocytopenic purpura (ITP), microscopic
 289 polyangiitis (MPA)

290 *** hydroxychloroquine

291 **** defined as malignancy requiring treatment in the last six months; one patient with papillary thyroid
 292 cancer requiring thyroidectomy, no systemic treatment required

293

294 There were eight HD subjects who previously tested positive for SARS-CoV-2, with positive test dates
 295 ranging from 7 months to four weeks preceding vaccination. Five control subjects self-reported a prior
 296 positive SARS-CoV-2 test, with positive test dates ranging from 8 months to four weeks preceding

297 vaccination. Detailed clinical characterization of HD subjects is summarized in **Table 2**. Notable
298 laboratory data includes an elevated ferritin from normal (with high population variance), and anemia.

299 **Table 2. Baseline clinical lab values for maintenance hemodialysis patients.**

300

	Normal range	Mean (SD)
Kidney/HD status		
Urea Reduction Ratio (URR)	-	0.74 (0.052)
Months on HD	-	46 (44)
Iron		
Ferritin (ng/ml)	10 - 259	838 (550) *
% Transferrin saturation	25 - 50	38 (13)
Albumin	3.4 – 5	4.1 (0.40)
CBC		
WBCs (k/ul)	3.9 - 12	6.0 (2.1)
Hgb (g/dl)	13.2 – 18	10.5 (1.5) *
Lymphocytes (k/ul)	1.3 - 4.2	1.5 (0.7)
Neutrophils (k/ul)	1.3 - 7.5	3.7 (1.5)
Monocytes (k/ul)	0.4 - 1	0.5 (0.2)
Eosinophils (k/ul)	0.2 - 0.5	0.2 (0.2)

301 * indicates value outside of normal range

302

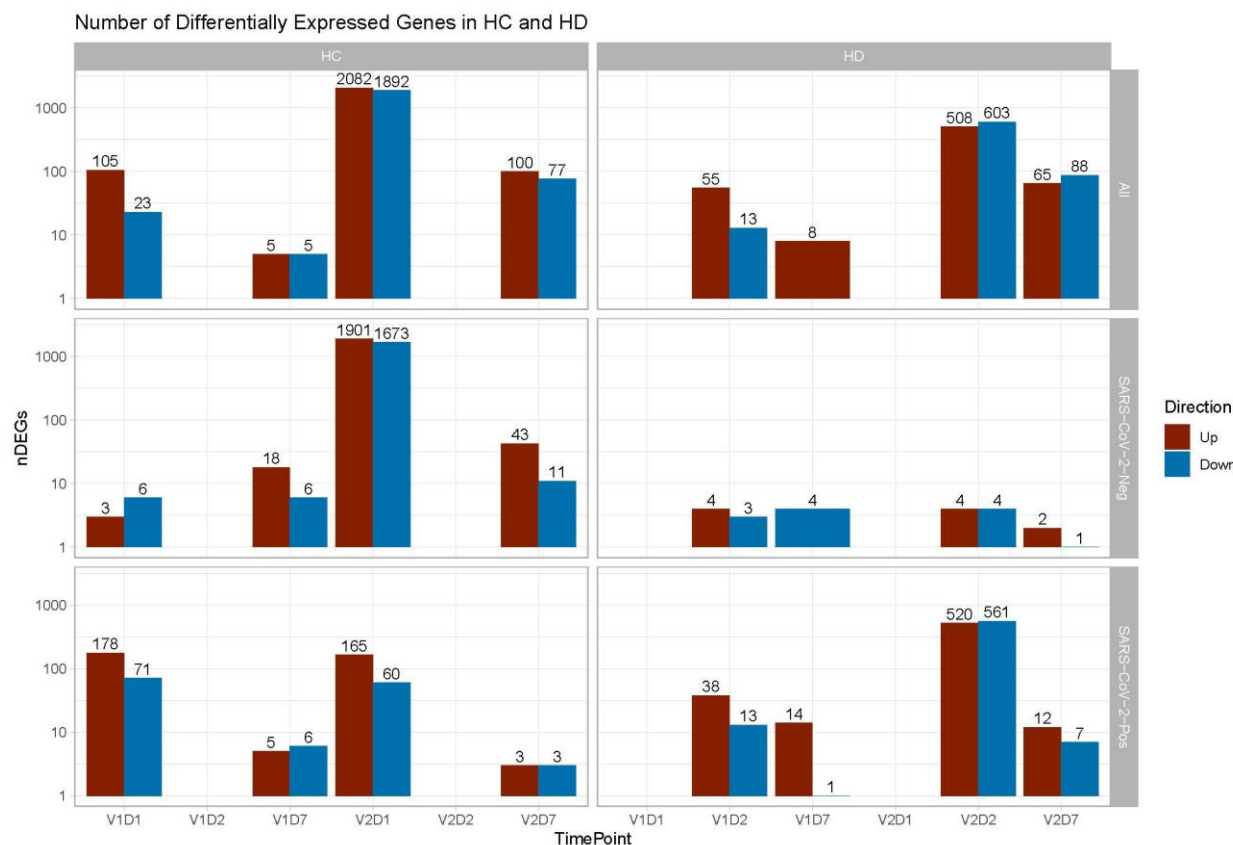
303 All subjects received two BTN162b2 vaccination doses with the second dose (V2) administered three
304 weeks after the first (V1). Anti-spike IgG binding and neutralizing assay data were obtained for all
305 subjects prior to V1 (V1D0) and seven days after V2 (V2D7). RNA sequencing data was obtained for all
306 control subjects prior to each vaccination dose (D0), and at one day (D1) and seven days (D7) after each
307 dose, corresponding to six time points: V1D0, V1D1, V1D7, V2D0, V2D1, V2D7. One control subject is
308 missing V2D0 data, and one is missing V2D1 data. RNA sequencing data was obtained for 12 HD subjects
309 prior to each vaccination dose, and at two days (D2) and seven days after each dose, corresponding to
310 six time points: V1D0, V1D2, V1D7, V2D0, V2D2, V2D7. Two HD subjects are missing V2D2 data.
311 Sequencing data was not obtained for subjects with fewer than five time points of successfully
312 constructed RNA libraries, due to time points without sample collection or failure to extract high quality

313 mRNA from PBMCs. Six-month follow-up (M6) anti-Spike IgG binding titers were obtained for 15 HC
314 subjects and 19 HD subjects. One HD subject tested positive for SARS-CoV-2 14 days after the second
315 vaccination dose, demonstrating mild symptoms. None of the other subjects reported SARS-CoV-2
316 infection up to 6 months follow up after the second vaccination.

317

318 *Differential Gene Expression Analysis*

319 To characterize the molecular basis of immune responses to vaccination in HC and HD, we performed
320 differential gene expression analyses of the PBMC RNA sequencing data. There are substantially more
321 differentially expressed genes (DEGs) in response to V2 compared to V1, and at D1 and D2 post-
322 vaccination compared to D7 (Figure 1). For HC, the largest number of DEGs is found at V2D1, indicating
323 the most transcriptional activity immediately after the 2nd vaccine dose, followed by V2D7, V1D1, and
324 V1D7. HD follows a similar pattern, with the largest number of DEGs found at V2D2, followed by V2D7,
325 V1D2, and V1D7. Notably, HD subjects with no SARS-CoV-2 history (n = 6) have substantially lower
326 numbers of DEGs than HD subjects with positive SARS-CoV-2 history (n = 6) at each time point, and
327 particularly at V2 time points.



328

329 **Figure 1. Differentially expressed genes (DEGs) increased after second vaccination dose compared to**

330 **first, and at Day 1 and 2 (D1/D2) compared to Day 7 (D7) for both controls (HC) and maintenance**

331 **hemodialysis (HD). Number of DEGs at each time point is displayed on a log scale, with DEGs for HC**

332 **shown for D1 and D7 compared to pre-vaccination time point (D0), and DEGs for HD shown for D2 and**

333 **D7 compared to D0. DEGs are shown independently of SARS-CoV-2 history (Top), for analysis of only**

334 **subjects with no prior SARS-CoV-2 history (Middle), and for analysis of only subjects with prior SARS-**

335 **CoV-2 history (Bottom). The DESeq2 R package was used to identify genes that were differentially**

336 **expressed at each time point after vaccination for each subject group ($p < 0.05$, FDR-adjusted).**

337

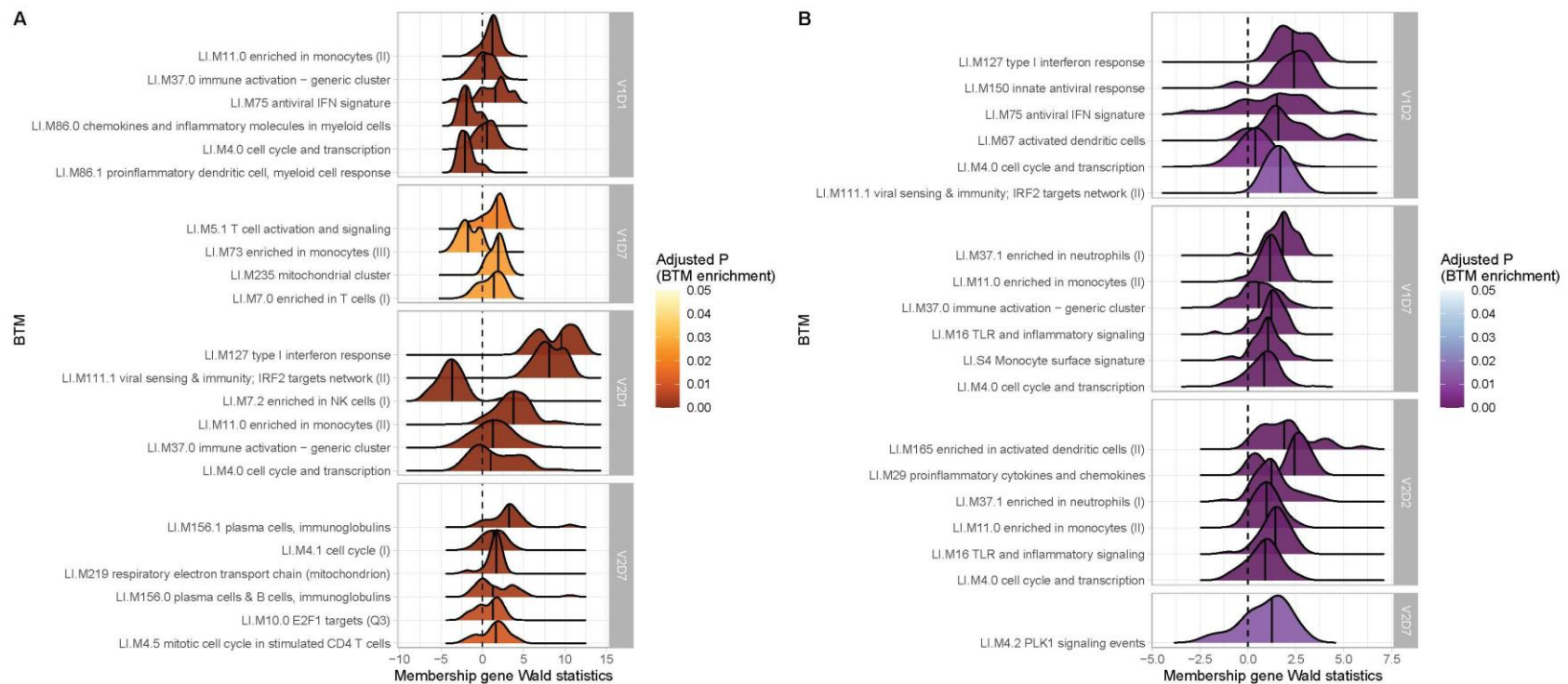
338 Direct comparison of gene expression between HC and HD with no prior reported SARS-CoV-2 infection

339 at V1D7 yielded five DEGs in HD versus HC including increased expression of chemokine CCL19 in HD ($p <$

340 0.05, FDR-corrected). Comparison of these same groups at V2D7 yielded 18 DEGs including increased
341 expression in HD of TIA1, which encodes a granule-associated protein expressed in cytolytic
342 lymphocytes³⁰ and natural killer cells, and BH3, a pro-apoptotic Bcl-2 family member and mediator of
343 lymphocyte apoptosis³¹.

344 *Blood Transcription Module (BTM) Enrichment*

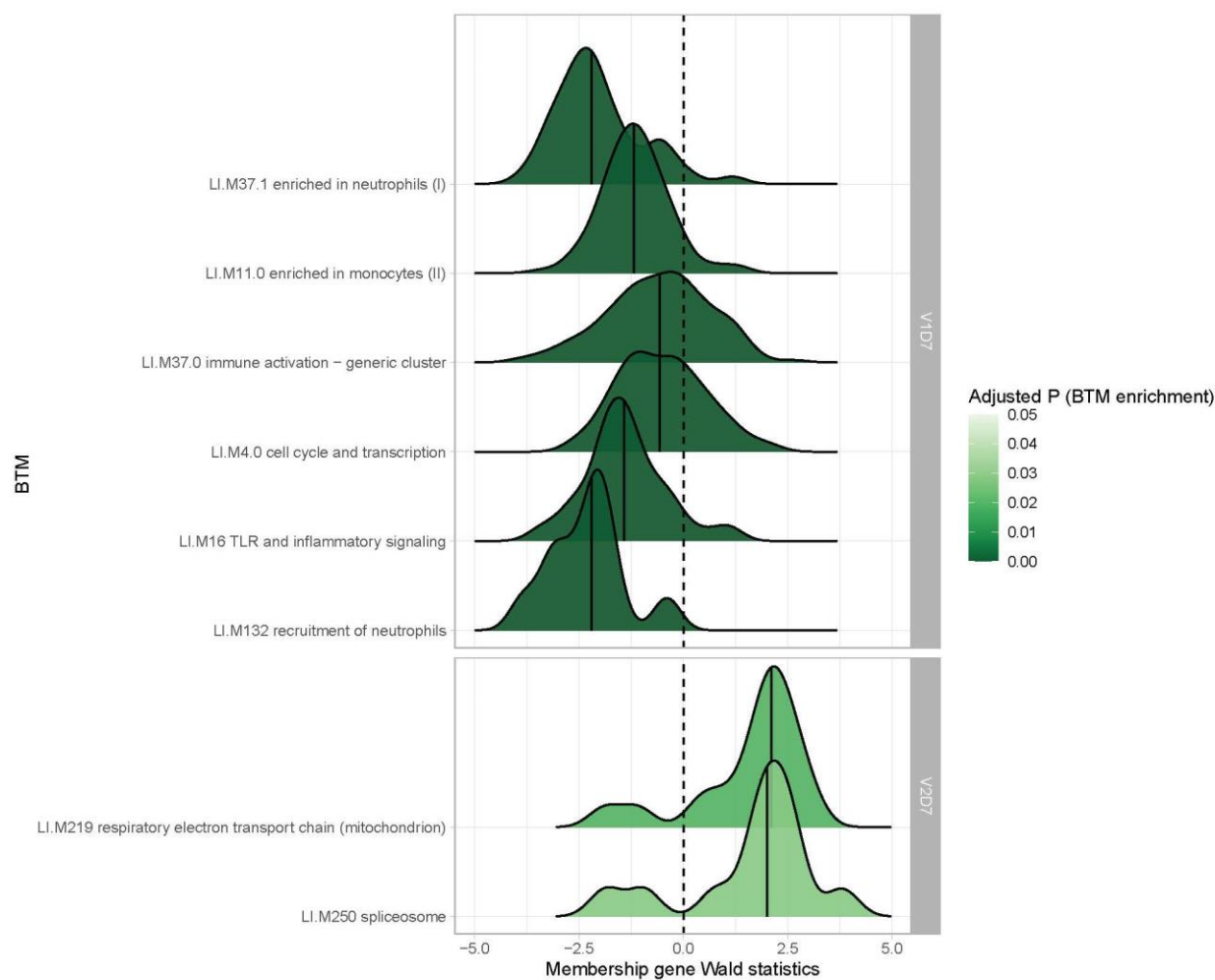
345 BTM enrichment analysis of subjects without SARS-CoV-2 history reveals the vaccine-induced
346 progression of various immune processes at each time point after vaccination (Figure 2). Following V1,
347 HC demonstrate early (V1D1) enrichment of 29 BTMs, with substantial upregulation of monocyte and
348 antiviral IFN activity (**TableS1**). The immune response transitions to V1D7 enrichment of four BTMs
349 including significant T cell activation and downregulation of monocytes (**TableS2**). Following V2, HC
350 demonstrate early (V2D1) enrichment of 82 BTMs, with substantial upregulation of innate antiviral
351 activity, similarly to V1D1 (**TableS3**). The immune response transitions to V2D7 enrichment of ten BTMs,
352 with significant upregulation of plasma cells and immunoglobulins (**TableS4**).



354

355 **Figure 2. Controls (HC) and maintenance hemodialysis subjects (HD) with no SARS-CoV-2 history demonstrate differing longitudinal**
 356 **enrichments of blood transcription modules (BTMs).** (A) The most significantly enriched BTMs are shown (up to six) for Day 1 (D1) and Day 7
 357 (D7) after each vaccination dose (V1, V2) in HC with no prior infection with SARS-CoV-2 ($p < 0.05$, FDR-adjusted). Density plots for each BTM
 358 represent Wald statistics from DESeq2 analysis for each membership gene, thereby representing increased or decreased expression per gene at
 359 each time point compared to baseline (V1D0 or V2D0). (B) Similarly to (A), the most significantly enriched BTMs for Day 2 (D2) and Day 7 (D7) in
 360 HD are shown.

361 In contrast, HD demonstrate early (V1D2) enrichment of 12 BTMs after the first vaccination dose, most
362 significantly involving upregulation of innate antiviral responses (**Figure 2, TableS5**). The immune
363 response transitions to V1D7 enrichment of 17 BTMs, with substantial upregulation of myeloid modules
364 (**Figure 2, TableS6**). The V1D7 positive enrichment of monocyte/myeloid modules in HD contrast the
365 negative enrichment of these modules in HC (**Figure 2, Figure S1**). Following the second vaccination
366 dose, HD demonstrate early (V2D2) enrichment of 27 BTMs most significantly involving upregulation of
367 dendritic cell activity and proinflammatory cytokines and chemokines (**Figure3, TableS7**). The immune
368 response progresses to V2D7 enrichment of one BTM: PLK signaling events (**Figure 2**).

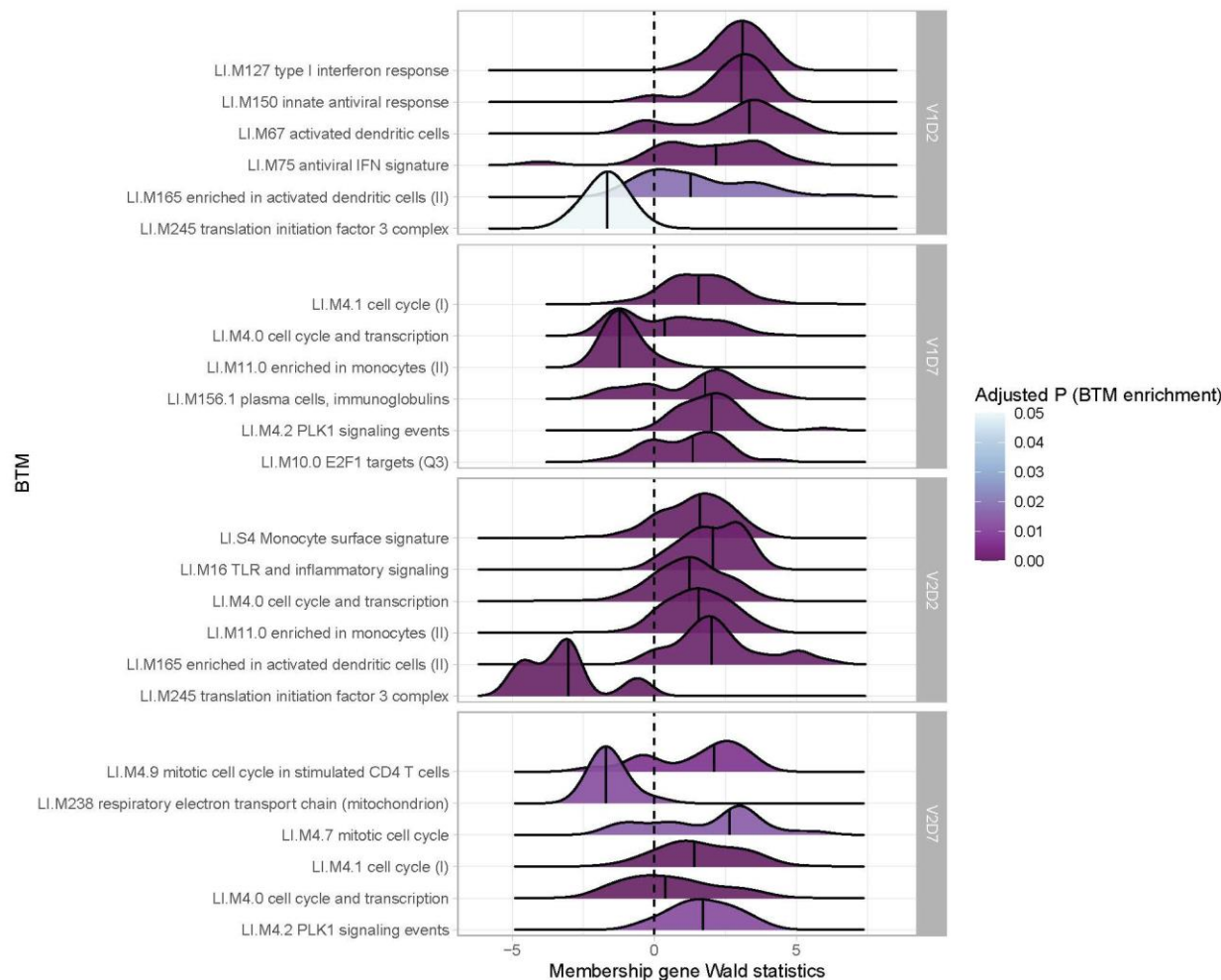


369

370 **Figure S1. Hemodialysis patients (HD) without prior SARS-CoV-2 infection show increased myeloid**
371 **activity at V1D7 and decreased metabolic activity at V2D7 compared to controls (HC).** The most
372 differentially enriched blood transcription modules (BTMs) between HC and HD with no prior infection
373 with SARS-CoV-2 are shown ($p < 0.05$, FDR-adjusted) at V1D7 and at one week after second vaccination
374 dose (V2D7). Density plots for each BTM represent Wald statistics from DESeq2 analysis for each
375 membership gene per BTM, with positive Wald statistics indicating increased expression in HC compared
376 to HD.

377

378 While there were no significant BTM enrichments in HC with positive SARS-CoV-2 history, most likely
379 due to the insufficient number of subjects, BTM enrichments for HD with positive SARS-CoV-2
380 demonstrated notable upregulation of plasma cell activity at V1D7. This contrasts with V1D7 for HD with
381 negative SARS-CoV-2, which show primary enrichment of myeloid BTMs (**Figure 2**). The remainder of
382 these enrichments are shown in **Figure S2**.



383

384 **Figure S2. Hemodialysis patients (HD) with prior SARS-CoV-2 infection show increased expression of**

385 **innate and adaptive immune blood transcription modules (BTMs) post-vaccination.** The most

386 significantly enriched BTMs are shown (up to six) for Day 2 (D2) and Day 7 (D7) after each vaccination

387 dose (V1, V2) in HD with prior infection with SARS-CoV-2 ($p < 0.05$, FDR-adjusted). Density plots for each

388 BTM represent Wald statistics from DESeq2 analysis for each membership gene, thereby representing

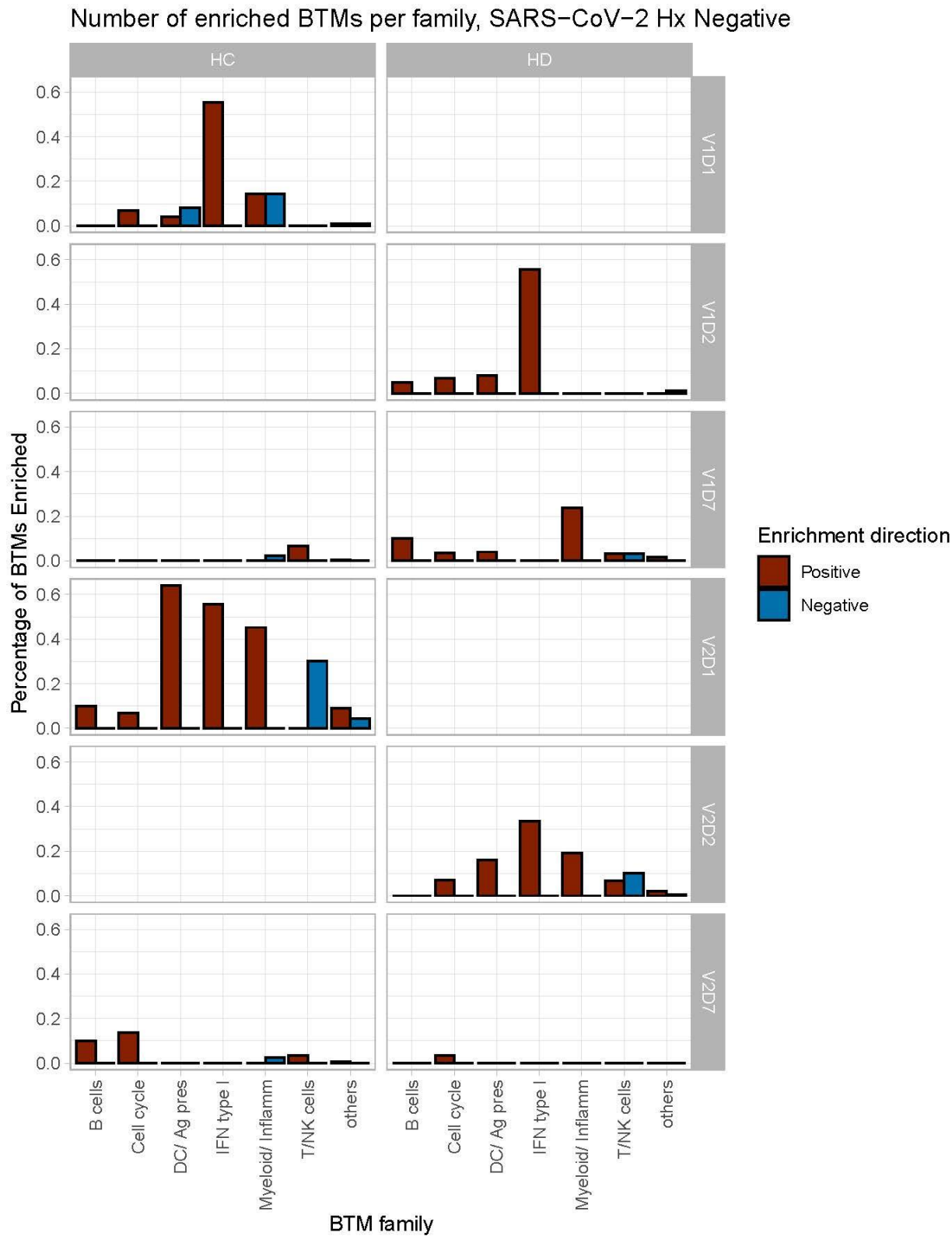
389 increased or decreased expression per gene at each time point compared to baseline (V1D0 or V2D0).

390

391 Summary enrichments using BTM families show many positive early V1 enrichments of Type 1 IFN

392 activity that dissipate by V1D7 in both HC and HD (**Figure 3**). However, HC show early positive and

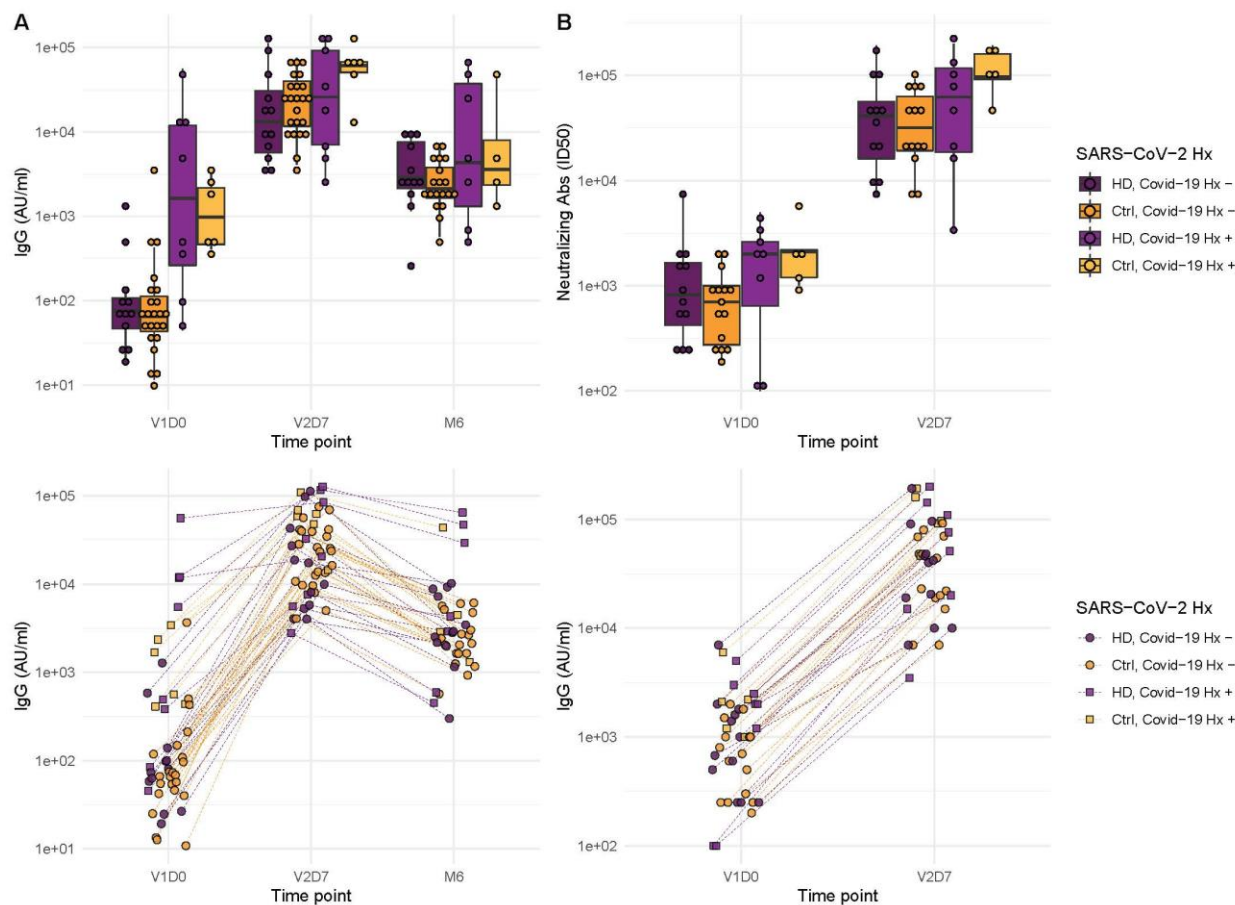
393 negative enrichments of myeloid/inflammatory family activity that dissipate by V1D7, while HD show
394 many early positive enrichments of myeloid/inflammatory family activity that persist and increase at
395 V1D7. Following V2, HC show early predominance of dendritic cell (DC)/antigen presenting cell (APC),
396 IFN Type I, and myeloid/inflammatory family activity transitioning to B cell and cell cycle activity at
397 V2D7, while HD show predominant early IFN type I family activity transitioning to just one detectable
398 cell cycle module enrichment.



400 **Figure 3. Controls (HC) and maintenance hemodialysis subjects (HD) demonstrate differing time**
401 **courses of blood transcription module (BTM) enrichment after each vaccination dose.** Percentage of
402 BTMs in each BTM family with significant enrichment at each time point after each vaccination dose (V1,
403 V2) for Day 1 (D1) and Day 7 (D7) in HC, and Day 2 (D2) and D7 for HD in subjects with no prior infection
404 with SARS-CoV-2 ($p < 0.05$, FDR-adjusted). Direction of enrichment was determined using the median
405 Wald statistic from DESeq2 analysis for each BTM membership gene, thereby representing overall
406 increased or decreased expression of membership genes at each time point compared to baseline (V1D0
407 or V2D0).

408 *Antibody Binding and Neutralization Assay Response*

409 We next aimed to assess immune protection conferred by the vaccine through quantification of anti-
410 spike IgG antibodies and functional assessment of neutralizing antibodies. All subjects demonstrated an
411 increase in anti-spike IgG at V2D7, with titers for all subjects except one still elevated above baseline at
412 six months. The exception was one HD subject with prior SARS-CoV-2 infection who demonstrated the
413 highest baseline titers of all subjects prior to vaccination. Both HC and HD subjects demonstrated a
414 statistically significant increase in anti-spike IgG and neutralization activity (ID50) from V1D0 to V2D7 (p
415 < 0.001), followed by an expected decrease at M6 from V2D7 levels ($p < 0.001$) (**Figure 4**). Despite this
416 decrease, M6 titers were still increased compared to baseline ($p < 0.001$).



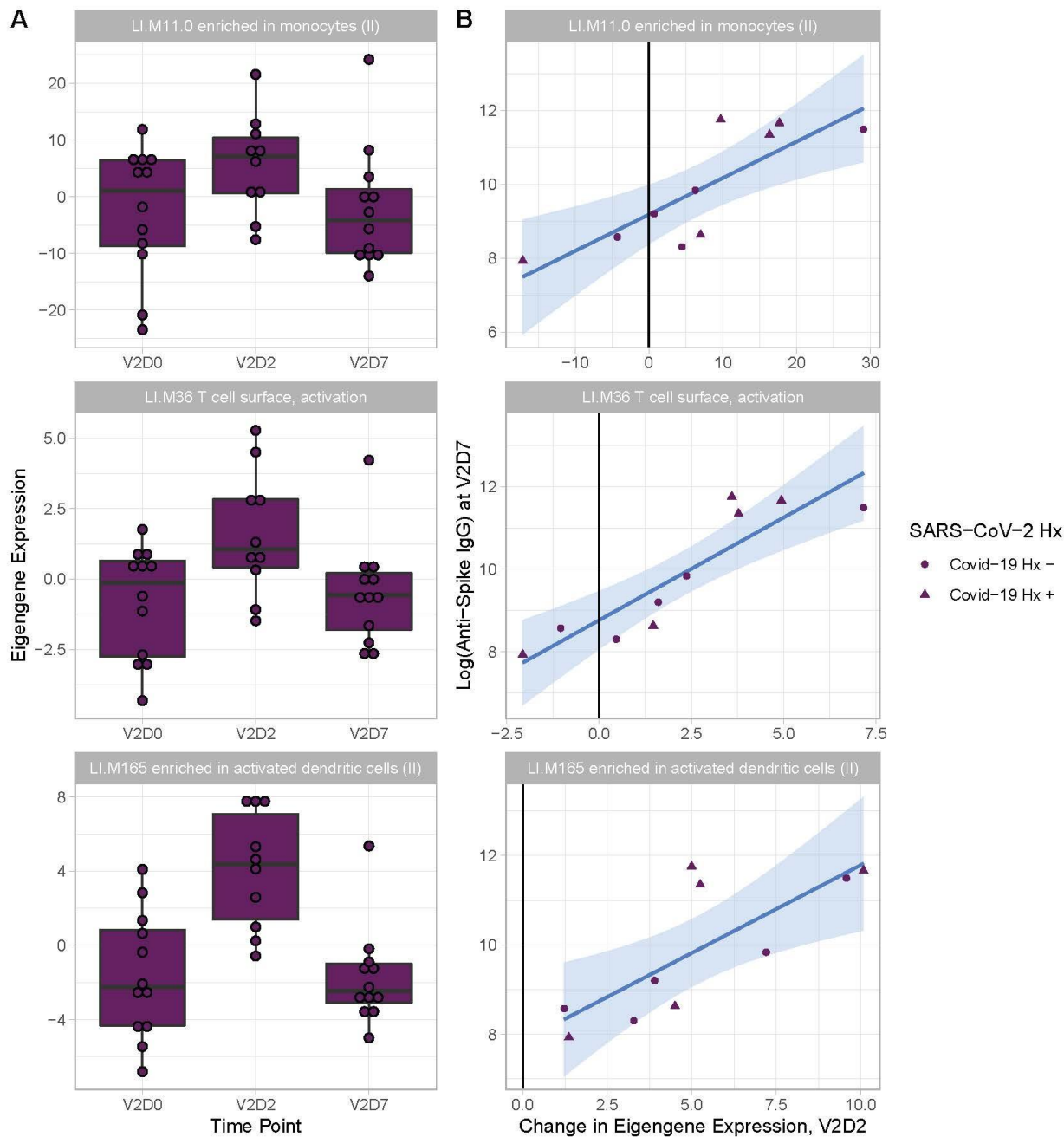
417
418 **Figure 4. Antibodies significantly increased in controls and maintenance hemodialysis (HD) one week**
419 **after the second vaccination dose ($p < 0.001$) and six months after initial vaccination ($p < 0.001$) with**
420 **the BNT162b2 mRNA COVID-19 vaccine. (A) Anti-spike IgG levels in controls and HD subjects with and**
421 **without prior SARS-CoV-2 history before vaccination (V1D0), one week after second vaccination dose**
422 **(V2D7), and six months after initial vaccination (M6). (B) Antibody neutralization activity (ID50) in**
423 **controls and HD subjects with and without prior SARS-CoV-2 history at V1D0 and V2D7.**
424
425 Higher anti-spike IgG at V2D7 was significantly predicted by higher pre-vaccination anti-spike IgG,
426 control group assignment, and younger age ($p < 0.01$, $p < 0.05$, $p < 0.05$, respectively), while gender, race,
427 and ethnicity were not. Higher anti-spike IgG at M6 was significantly predicted by higher V2D7 anti-spike

428 IgG ($p < 0.001$), with no additional predictive value conferred by SARS-CoV-2 history, subject group, age,
429 gender, race, or ethnicity. Higher neutralization activity (ID50) at V2D7 was significantly predicted by
430 higher pre-vaccination ID50, with no additional predictive value conferred by subject group, age, gender,
431 race, and ethnicity.

432

433 *Transcriptomic and clinical predictors of antibody binding response in HD*

434 Linear models to predict anti-Spike IgG at V2D7 and at M6 in HD using enriched BTMs, controlling for
435 SARS-CoV-2 history, identified BTM predictors at all time points except for V1D2. Of the 18 enriched
436 BTMs at V1D7, increased expression (from V1D0) of “LI.M156.1 plasma cells, immunoglobulins” was
437 predictive of higher anti-spike IgG at V2D7 ($p < 0.05$, FDR-corrected), controlling for SARS-CoV-2 history.
438 Of the 30 enriched BTMs at V2D2, increased expression of 18 BTMs was predictive of higher anti-Spike
439 IgG at V2D7 ($p < 0.05$, FDR-corrected). These include innate immune, antigen presentation, and T cell
440 pathways (**Figure 5**). Increased expression of “LI.M4.2 PLK1 signaling events” at V2D7 compared to
441 V2D0, which was the only enriched module at this time point for HD subjects with no SARS-CoV-2
442 history, was predictive of higher anti-spike IgG at both V2D7 and M6 ($p < 0.05$).



443

444 **Figure 5. Increased expression of multiple Blood Transcription Modules (BTMs) at V2D2 is predictive**

445 **of higher anti-spike IgG at V2D7.** Of 30 enriched BTMs at V2D2, increased expression of 18 BTMs is

446 predictive of increased anti-spike IgG at V2D7 ($p < 0.05$, FDR-corrected), controlling for SARS-CoV-2

447 history. Predictive pathways include innate immune, antigen presentation, and T cell pathways. Three

448 examples are shown.

449

450 Linear models to predict anti-Spike IgG at V2D7 and at M6 in HD using clinical predictors yielded

451 significant baseline and post-vaccination predictors. Baseline ferritin levels in the intermediate range

452 (200 – 2000 ng/ml) were associated with higher anti-spike IgG at V2D7 and M6 ($p < 0.01$, $p < 0.05$),

453 controlling for history of SARS-CoV-2. URR, WBC counts, transferrin saturation, and hemoglobin were

454 not significant predictors of antibody development. **Figure 6A** shows anti-spike IgG at V2D7 as a function

455 of baseline ferritin levels, identifying the intermediate range of ferritin which has previously been

456 associated with lowest all-cause mortality²⁰

457 The LFC of WBCs from baseline after the first vaccination dose was significantly predictive of antibody

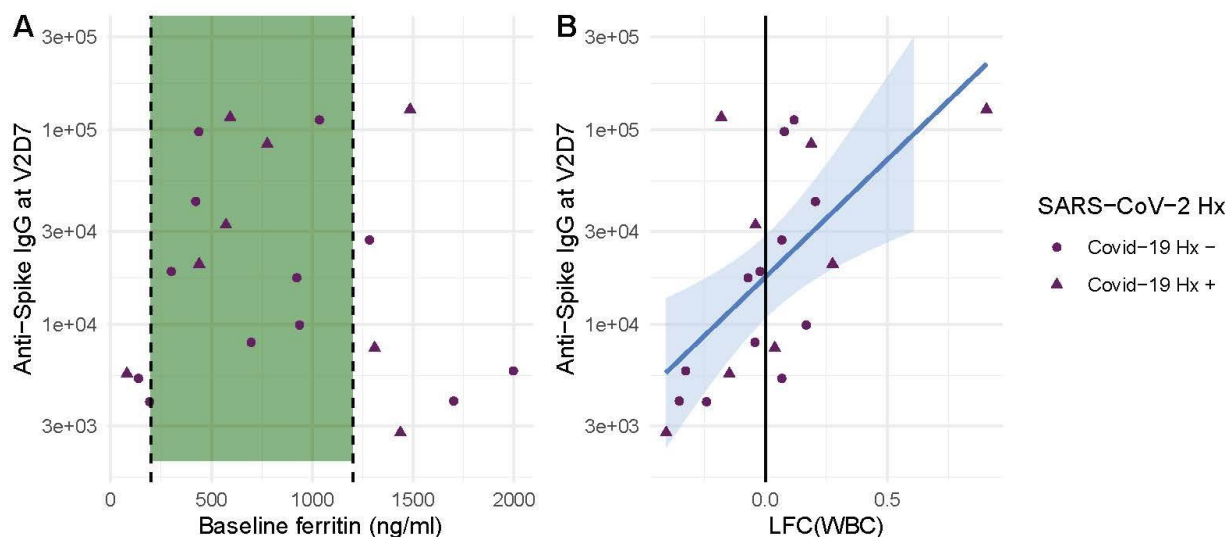
458 titer levels at both V2D7 ($p < 0.01$) and M6 ($p < 0.05$), controlling for SARS-CoV-2 history and number of

459 days after vaccination that labs were collected (**Figure 6B**). The predictive value of LFC of WBCs is

460 predominantly driven by increased lymphocyte counts; LFC of absolute lymphocyte counts was

461 predictive of V2D7 ($p < 0.01$) and M6 (trend-level, $p = 0.056$) antibody titers, controlling for initial

462 antibody titers and date of clinical labs.



463

464 **Figure 6. Baseline ferritin level and post-V1 white blood cell count (WBC) are clinical predictors of**
465 **post-V2 antibody responses in maintenance hemodialysis patients (HD).** (A) Ferritin levels associated
466 with lowest all-cause mortality predict the development of higher anti-spike IgG after vaccination at
467 V2D7 ($p < 0.01$) and M6 (not shown, $p < 0.05$) in maintenance HD patients. Dashed vertical lines indicate
468 the intermediate range of ferritin (200-1200 ng/ml) associated with lowest all-cause mortality ²⁰. (B)
469 Increased WBC after first vaccination dose is predictive of anti-spike IgG titers after vaccination at V2D7
470 ($p < 0.01$) and M6 (not shown, $p < 0.05$) in maintenance HD patients. Points with negative log-fold
471 change of white blood cell counts (LFC(WBC)) and positive LFC(WBC) represent a decrease and increase,
472 respectively, in WBC from baseline labs.

473

474 **Discussion**

475 Our results demonstrate differing expression of BTMs and differing time courses of immune responses
476 to the BTN162b2 mRNA COVID-19 vaccination in maintenance hemodialysis subjects (HD) compared to
477 controls. Controls demonstrated expected transitions from early Type I interferon and myeloid activity
478 to T cell activity after the first vaccination dose (**Figure 2, Figure 3**). The predominant positive
479 enrichment of T cell modules in controls at one week after the first vaccination dose (V1D7) was
480 contrasted with predominant positive enrichment of myeloid modules in HD at V1D7. Interestingly, HD
481 showed prolonged upregulation of myeloid activity at V1D7, while controls showed downregulation of
482 these modules at V1D7 (**Figure 2, Figure S1**). Overall, these observations indicate delayed resolution of
483 innate myeloid responses in the HD cohort.

484 Following the second vaccination dose, both groups demonstrated early enrichment of innate immune
485 modules, with HC alone transitioning to a plasma cell response by V2D7 (**Figure 3**). Direct group
486 comparisons at V2D7 did not show differences of plasma cell response, but metabolic activity was

487 decreased in HD compared to controls (**Figure S1**). Further, HD demonstrated increased V2D7
488 expression compared to controls of pro-apoptotic Bcl-2 family member BH3, a mediator of lymphocyte
489 apoptosis. A prior study showed accelerated *in vitro* apoptosis of lymphocytes in uremia, with a
490 particularly pronounced effect on B cells, mediated by dysregulation of Bcl-2. These results suggest a
491 state of heightened cellular stress in HD after vaccination leading to increased apoptotic signaling.

492 Despite differing transcriptomic time courses in the two group, our results demonstrate significant
493 elevation of anti-spike IgG titers after two doses of BNT162b2 mRNA COVID-19 vaccination in both HD
494 and controls. HD demonstrated only a slight decrease of IgG levels at V2D7 when controlling for SARS-
495 CoV-2 history ($p < 0.05$) and no statistically significant difference at six months. Prior studies comparing
496 short-term antibody response to BNT162b2 mRNA COVID-19 vaccination in HD versus controls find
497 antibody response rates of 84-96% in HD after two vaccination doses, but with lower mean IgG levels
498 compared to controls^{16-19,32-34}. Notably, the HD population studied here is younger and more racially
499 and ethnically diverse. The average age of HD cohorts in prior studies was predominantly in the 60s,
500 compared to an average age of 54 in our study. Jahn et al. found in a subset analysis that HD patients
501 under 60 years of age responded equally to healthy controls, suggesting an interaction between
502 increasing age and less effective antibody response in HD patients¹⁷.

503 HD subjects with documented SARS-CoV-2 infection prior to vaccination had wider variance of antibody
504 titers at all time points in this study, with two subjects demonstrating V1D0 antibody titer levels similar
505 to that of uninfected subjects. These two subjects consistently had the lowest titer levels at V2D7 and
506 M6 within the group of previously infected subjects and amongst the lowest titers across all subjects.
507 One subject is the oldest enrolled patient, and both are diagnosed with hyperlipidemia.

508 Given previously and presently demonstrated the wider variance of protective immune responses in HD
509 and altered interactions with risk factors including age, it is valuable to identify predictors of the

510 strength of immune response to vaccination in this population. We identified both transcriptomic and
511 clinical predictors of anti-spike IgG development at both V2D7 and six months after the second
512 vaccination dose (M6). Increased gene expression of blood transcription modules (BTMs) including
513 monocyte activity, dendritic cell and antigen presentation activity, IFN type I activity, and T cell
514 activation two days after the second vaccination dose (V2D2) in HD were predictive of V2D7 anti-spike
515 IgG. Additionally, increased expression of PLK1 signaling events, indicating increased cell cycle activity, at
516 V2D7 was predictive of V2D7 and M6 anti-spike IgG. Clinically, serum ferritin values in the intermediate
517 range at baseline predicted stronger anti-spike IgG development. A prior study of 58,058 maintenance
518 HD subjects found serum ferritin levels between 200 and 1200 ng/ml to be associated with lower all-
519 cause mortality, due to ferritin <200 ng/ml representing low iron status, and >1200 ng/ml representing a
520 hyper-inflammatory state due to ferritin's status as an acute phase reactant²⁰. Iron deficiency has been
521 linked to impaired immune response and vaccine efficacy in other infections, while inflammation
522 induces macrophage release of the heavy chain component of ferritin, FTH, which has been reported to
523 inhibit lymphocyte proliferation and function^{34,35}. Additionally, increased LFC in WBC count 1-3 weeks
524 after vaccination was predictive of higher antibody titers.

525 Our study is limited by different early time points between controls and HD (Day 1 vs Day 2 after each
526 vaccination dose) and by sample size, particularly when subdividing SARS-CoV-2 history. The smaller
527 sample size additionally limits our ability to characterize differential immune pathways in clinical subsets
528 of the dialysis population, such as those with low, medium, and high baseline ferritin levels. Future
529 studies are needed for more comprehensive characterization of the immune pathway recruitment in
530 response to the Covid-19 vaccinations in this population. The Covid-19 mRNA vaccines are proving more
531 efficacious than other vaccines in the ESRD population; for example, while more than 90% of patients
532 without chronic kidney disease develop protective antibodies against hepatitis B after vaccination, only
533 50-60% of patients with ESRD seroconvert⁹. One explanation is that, in mRNA vaccines, the mRNA both

534 encodes the viral antigen and acts as an adjuvant due to its innate immunostimulatory properties; the
535 mRNA is recognized by endosomal and cytosolic innate sensors upon cell entry, resulting in cellular
536 activation and production of type I interferons and other inflammatory mediators³⁶. This elevated
537 innate immune stimulus could overcome immune desensitization in ESRD, evidenced by diminished
538 TLR4 expression on monocytes³⁷ and downregulation of activating receptors on natural killer cells in this
539 population³⁸. If so, the mRNA vaccine delivery vehicle could prove particularly valuable in vaccine
540 development for ESRD and HD going forward.

541 Overall, we demonstrate differing time courses of immune responses to the BTN162b2 mRNA COVID-19
542 vaccination in maintenance hemodialysis subjects (HD) and identify transcriptomic and clinical
543 predictors of anti-Spike IgG titers in HD. Given the efficacy of this vaccination in our HD cohort, the
544 differential transcriptomic responses likely represent immune alterations with sub-clinical effects on
545 humoral immune response to the BTN162b2 mRNA COVID-19 vaccine. Our results warrant further
546 characterization of the immune dysregulation of ESRD and of immune biomarkers that underlie
547 efficacious immune responses to vaccination in this population.

548

549 Mendeley references

- 550 1. Johansen KL, Chertow GM, Gilbertson DT, et al. US Renal Data System 2021 Annual Data Report:
551 Epidemiology of Kidney Disease in the United States. *American journal of kidney diseases : the*
552 *official journal of the National Kidney Foundation*. 2022;79(4 Suppl 1):A8-A12.
553 doi:10.1053/j.ajkd.2022.02.001
- 554 2. Williams JD, Topley N, Craig KJ, et al. The Euro-Balance Trial: the effect of a new biocompatible
555 peritoneal dialysis fluid (balance) on the peritoneal membrane. *Kidney Int*. 2004;66(1):408-418.
556 doi:10.1111/j.1523-1755.2004.00747.x
- 557 3. Kato S, Chmielewski M, Honda H, et al. Aspects of immune dysfunction in end-stage renal
558 disease. *Clin J Am Soc Nephrol*. 2008;3(5):1526-1533. doi:10.2215/CJN.00950208
- 559 4. Satomura A, Endo M, Ohi H, et al. Significant elevations in serum mannose-binding lectin levels in
560 patients with chronic renal failure. *Nephron*. 2002;92(3):702-704. doi:10.1159/000064089

- 561 5. Lim WH, Kireta S, Leedham E, Russ GR, Coates PT. Uremia impairs monocyte and monocyte-
562 derived dendritic cell function in hemodialysis patients. *Kidney Int.* 2007;72(9):1138-1148.
563 doi:10.1038/sj.ki.5002425
- 564 6. Fernández-Fresnedo G, Ramos MA, González-Pardo MC, de Francisco AL, López-Hoyos M, Arias
565 M. B lymphopenia in uremia is related to an accelerated in vitro apoptosis and dysregulation of
566 Bcl-2. *Nephrology, dialysis, transplantation : official publication of the European Dialysis and
567 Transplant Association - European Renal Association.* 2000;15(4):502-510.
568 doi:10.1093/ndt/15.4.502
- 569 7. Stenvinkel P, Ketteler M, Johnson RJ, et al. IL-10, IL-6, and TNF-alpha: central factors in the
570 altered cytokine network of uremia--the good, the bad, and the ugly. *Kidney Int.*
571 2005;67(4):1216-1233. doi:10.1111/j.1523-1755.2005.00200.x
- 572 8. Ghadiani MH, Besharati S, Mousavinasab N, Jalalzadeh M. Response rates to HB vaccine in CKD
573 stages 3-4 and hemodialysis patients. *Journal of research in medical sciences : the official journal
574 of Isfahan University of Medical Sciences.* 2012;17(6):527-533.
- 575 9. Eleftheriadis T, Antoniadi G, Liakopoulos V, Kartsios C, Stefanidis I. Disturbances of acquired
576 immunity in hemodialysis patients. *Semin Dial.* 2007;20(5):440-451. doi:10.1111/j.1525-
577 139X.2007.00283.x
- 578 10. Scherer A, Günther OP, Balshaw RF, et al. Alteration of human blood cell transcriptome in
579 uremia. *BMC Med Genomics.* 2013;6:23. doi:10.1186/1755-8794-6-23
- 580 11. Granata S, Zaza G, Simone S, et al. Mitochondrial dysregulation and oxidative stress in patients
581 with chronic kidney disease. *BMC Genomics.* 2009;10:388. doi:10.1186/1471-2164-10-388
- 582 12. Liu Y, Fiskum G, Schubert D. Generation of reactive oxygen species by the mitochondrial electron
583 transport chain. *J Neurochem.* 2002;80(5):780-787. doi:10.1046/j.0022-3042.2002.00744.x
- 584 13. Zaza G, Pontrelli P, Pertosa G, et al. Dialysis-related systemic microinflammation is associated
585 with specific genomic patterns. *Nephrology, dialysis, transplantation : official publication of the
586 European Dialysis and Transplant Association - European Renal Association.* 2008;23(5):1673-
587 1681. doi:10.1093/ndt/gfm804
- 588 14. Baden LR, El Sahly HM, Essink B, et al. Efficacy and Safety of the mRNA-1273 SARS-CoV-2 Vaccine.
589 *N Engl J Med.* 2021;384(5):403-416. doi:10.1056/NEJMoa2035389
- 590 15. Polack FP, Thomas SJ, Kitchin N, et al. Safety and Efficacy of the BNT162b2 mRNA Covid-19
591 Vaccine. *N Engl J Med.* 2020;383(27):2603-2615. doi:10.1056/NEJMoa2034577
- 592 16. Grupper A, Sharon N, Finn T, et al. Humoral Response to the Pfizer BNT162b2 Vaccine in Patients
593 Undergoing Maintenance Hemodialysis. *Clin J Am Soc Nephrol.* 2021;16(7):1037-1042.
594 doi:10.2215/CJN.03500321
- 595 17. Jahn M, Korth J, Dorsch O, et al. Humoral Response to SARS-CoV-2-Vaccination with BNT162b2
596 (Pfizer-BioNTech) in Patients on Hemodialysis. *Vaccines (Basel).* 2021;9(4).
597 doi:10.3390/vaccines9040360

- 598 18. Attias P, Sakhi H, Rieu P, et al. Antibody response to the BNT162b2 vaccine in maintenance
599 hemodialysis patients. *Kidney Int.* 2021;99(6):1490-1492. doi:10.1016/j.kint.2021.04.009
- 600 19. Anand S, Montez-Rath ME, Han J, et al. Antibody Response to COVID-19 vaccination in Patients
601 Receiving Dialysis. *medRxiv*. Published online May 2021. doi:10.1101/2021.05.06.21256768
- 602 20. Kalantar-Zadeh K, Regidor DL, McAllister CJ, Michael B, Warnock DG. Time-dependent
603 associations between iron and mortality in hemodialysis patients. *J Am Soc Nephrol.*
604 2005;16(10):3070-3080. doi:10.1681/ASN.2005040423
- 605 21. Chen S, Zhou Y, Chen Y, Gu J. fastp: an ultra-fast all-in-one FASTQ preprocessor. *Bioinformatics.*
606 2018;34(17):i884-i890. doi:10.1093/bioinformatics/bty560
- 607 22. Patro R, Duggal G, Love MI, Irizarry RA, Kingsford C. Salmon provides fast and bias-aware
608 quantification of transcript expression. *Nat Methods.* 2017;14(4):417-419.
609 doi:10.1038/nmeth.4197
- 610 23. Love MI, Sonesson C, Hickey PF, et al. Tximeta: Reference sequence checksums for provenance
611 identification in RNA-seq. *PLoS Comput Biol.* 2020;16(2):e1007664.
612 doi:10.1371/journal.pcbi.1007664
- 613 24. MATUMOTO M. A note on some points of calculation method of LD50 by Reed and Muench. *Jpn J*
614 *Exp Med.* 1949;20(2):175-179.
- 615 25. Nie J, Li Q, Wu J, et al. Quantification of SARS-CoV-2 neutralizing antibody by a pseudotyped
616 virus-based assay. *Nat Protoc.* 2020;15(11):3699-3715. doi:10.1038/s41596-020-0394-5
- 617 26. Ferrara F, Temperton N. Pseudotype Neutralization Assays: From Laboratory Bench to Data
618 Analysis. *Methods Protoc.* 2018;1(1). doi:10.3390/mps1010008
- 619 27. Pegu A, O'Connell SE, Schmidt SD, et al. Durability of mRNA-1273 vaccine-induced antibodies
620 against SARS-CoV-2 variants. *Science.* 2021;373(6561):1372-1377. doi:10.1126/science.abj4176
- 621 28. Li S, Rouphael N, Duraisingham S, et al. Molecular signatures of antibody responses derived from
622 a systems biology study of five human vaccines. *Nat Immunol.* 2014;15(2):195-204.
623 doi:10.1038/ni.2789
- 624 29. Braun RO, Brunner L, Wyler K, et al. System immunology-based identification of blood
625 transcriptional modules correlating to antibody responses in sheep. *NPJ Vaccines.* 2018;3:41.
626 doi:10.1038/s41541-018-0078-0
- 627 30. Anderson P, Nagler-Anderson C, O'Brien C, et al. A monoclonal antibody reactive with a 15-kDa
628 cytoplasmic granule-associated protein defines a subpopulation of CD8+ T lymphocytes. *J*
629 *Immunol.* 1990;144(2):574-582.
- 630 31. Labi V, Erlacher M, Kiessling S, et al. Loss of the BH3-only protein Bmf impairs B cell homeostasis
631 and accelerates gamma irradiation-induced thymic lymphoma development. *J Exp Med.*
632 2008;205(3):641-655. doi:10.1084/jem.20071658
- 633 32. Agur T, Ben-Dor N, Goldman S, et al. Antibody response to mRNA SARS-CoV-2 vaccine among
634 dialysis patients - a prospective cohort study. *Nephrology, dialysis, transplantation : official*

- 635 *publication of the European Dialysis and Transplant Association - European Renal Association.*
636 Published online April 2021. doi:10.1093/ndt/gfab155
- 637 33. Longlune N, Nogier MB, Miedougé M, et al. High immunogenicity of a messenger RNA-based
638 vaccine against SARS-CoV-2 in chronic dialysis patients. *Nephrology, dialysis, transplantation : official publication of the European Dialysis and Transplant Association - European Renal Association.* 2021;36(9):1704-1709. doi:10.1093/ndt/gfab193
639
640
- 641 34. Drakesmith H, Pasricha SR, Cabantchik I, et al. Vaccine efficacy and iron deficiency: an
642 intertwined pair? *Lancet Haematol.* 2021;8(9):e666-e669. doi:10.1016/S2352-3026(21)00201-5
- 643 35. Kernan KF, Carcillo JA. Hyperferritinemia and inflammation. *Int Immunol.* 2017;29(9):401-409.
644 doi:10.1093/intimm/dxx031
- 645 36. Teijaro JR, Farber DL. COVID-19 vaccines: modes of immune activation and future challenges. *Nat Rev Immunol.* 2021;21(4):195-197. doi:10.1038/s41577-021-00526-x
646
- 647 37. Koc M, Toprak A, Arikan H, et al. Toll-like receptor expression in monocytes in patients with
648 chronic kidney disease and haemodialysis: relation with inflammation. *Nephrology, dialysis, transplantation : official publication of the European Dialysis and Transplant Association - European Renal Association.* 2011;26(3):955-963. doi:10.1093/ndt/gfq500
649
650
- 651 38. Nagai K. Dysfunction of natural killer cells in end-stage kidney disease on hemodialysis. *Ren Replace Ther.* 2021;7(1):8. doi:10.1186/s41100-021-00324-0
652
653
- 654 1. Johansen KL, Chertow GM, Gilbertson DT, et al. US Renal Data System 2021 Annual Data Report:
655 Epidemiology of Kidney Disease in the United States. *American journal of kidney diseases : the official journal of the National Kidney Foundation.* 2022;79(4 Suppl 1):A8-A12.
656 doi:10.1053/j.ajkd.2022.02.001
657
- 658 2. Williams JD, Topley N, Craig KJ, et al. The Euro-Balance Trial: the effect of a new biocompatible
659 peritoneal dialysis fluid (balance) on the peritoneal membrane. *Kidney Int.* 2004;66(1):408-418.
660 doi:10.1111/j.1523-1755.2004.00747.x
- 661 3. Kato S, Chmielewski M, Honda H, et al. Aspects of immune dysfunction in end-stage renal
662 disease. *Clin J Am Soc Nephrol.* 2008;3(5):1526-1533. doi:10.2215/CJN.00950208
- 663 4. Satomura A, Endo M, Ohi H, et al. Significant elevations in serum mannose-binding lectin levels in
664 patients with chronic renal failure. *Nephron.* 2002;92(3):702-704. doi:10.1159/000064089
- 665 5. Lim WH, Kireta S, Leedham E, Russ GR, Coates PT. Uremia impairs monocyte and monocyte-
666 derived dendritic cell function in hemodialysis patients. *Kidney Int.* 2007;72(9):1138-1148.
667 doi:10.1038/sj.ki.5002425
- 668 6. Fernández-Fresnedo G, Ramos MA, González-Pardo MC, de Francisco AL, López-Hoyos M, Arias
669 M. B lymphopenia in uremia is related to an accelerated in vitro apoptosis and dysregulation of
670 Bcl-2. *Nephrology, dialysis, transplantation : official publication of the European Dialysis and*

- 671 *Transplant Association - European Renal Association*. 2000;15(4):502-510.
672 doi:10.1093/ndt/15.4.502
- 673 7. Stenvinkel P, Ketteler M, Johnson RJ, et al. IL-10, IL-6, and TNF-alpha: central factors in the
674 altered cytokine network of uremia--the good, the bad, and the ugly. *Kidney Int*.
675 2005;67(4):1216-1233. doi:10.1111/j.1523-1755.2005.00200.x
- 676 8. Ghadiani MH, Besharati S, Mousavinasab N, Jalalzadeh M. Response rates to HB vaccine in CKD
677 stages 3-4 and hemodialysis patients. *Journal of research in medical sciences : the official journal*
678 *of Isfahan University of Medical Sciences*. 2012;17(6):527-533.
- 679 9. Eleftheriadis T, Antoniadi G, Liakopoulos V, Kartsios C, Stefanidis I. Disturbances of acquired
680 immunity in hemodialysis patients. *Semin Dial*. 2007;20(5):440-451. doi:10.1111/j.1525-
681 139X.2007.00283.x
- 682 10. Scherer A, Günther OP, Balshaw RF, et al. Alteration of human blood cell transcriptome in
683 uremia. *BMC Med Genomics*. 2013;6:23. doi:10.1186/1755-8794-6-23
- 684 11. Granata S, Zaza G, Simone S, et al. Mitochondrial dysregulation and oxidative stress in patients
685 with chronic kidney disease. *BMC Genomics*. 2009;10:388. doi:10.1186/1471-2164-10-388
- 686 12. Liu Y, Fiskum G, Schubert D. Generation of reactive oxygen species by the mitochondrial electron
687 transport chain. *J Neurochem*. 2002;80(5):780-787. doi:10.1046/j.0022-3042.2002.00744.x
- 688 13. Zaza G, Pontrelli P, Pertosa G, et al. Dialysis-related systemic microinflammation is associated
689 with specific genomic patterns. *Nephrology, dialysis, transplantation : official publication of the*
690 *European Dialysis and Transplant Association - European Renal Association*. 2008;23(5):1673-
691 1681. doi:10.1093/ndt/gfm804
- 692 14. Baden LR, El Sahly HM, Essink B, et al. Efficacy and Safety of the mRNA-1273 SARS-CoV-2 Vaccine.
693 *N Engl J Med*. 2021;384(5):403-416. doi:10.1056/NEJMoa2035389
- 694 15. Polack FP, Thomas SJ, Kitchin N, et al. Safety and Efficacy of the BNT162b2 mRNA Covid-19
695 Vaccine. *N Engl J Med*. 2020;383(27):2603-2615. doi:10.1056/NEJMoa2034577
- 696 16. Grupper A, Sharon N, Finn T, et al. Humoral Response to the Pfizer BNT162b2 Vaccine in Patients
697 Undergoing Maintenance Hemodialysis. *Clin J Am Soc Nephrol*. 2021;16(7):1037-1042.
698 doi:10.2215/CJN.03500321
- 699 17. Jahn M, Korth J, Dorsch O, et al. Humoral Response to SARS-CoV-2-Vaccination with BNT162b2
700 (Pfizer-BioNTech) in Patients on Hemodialysis. *Vaccines (Basel)*. 2021;9(4).
701 doi:10.3390/vaccines9040360
- 702 18. Attias P, Sakhi H, Rieu P, et al. Antibody response to the BNT162b2 vaccine in maintenance
703 hemodialysis patients. *Kidney Int*. 2021;99(6):1490-1492. doi:10.1016/j.kint.2021.04.009
- 704 19. Anand S, Montez-Rath ME, Han J, et al. Antibody Response to COVID-19 vaccination in Patients
705 Receiving Dialysis. *medRxiv*. Published online May 2021. doi:10.1101/2021.05.06.21256768

- 706 20. Kalantar-Zadeh K, Regidor DL, McAllister CJ, Michael B, Warnock DG. Time-dependent
707 associations between iron and mortality in hemodialysis patients. *J Am Soc Nephrol*.
708 2005;16(10):3070-3080. doi:10.1681/ASN.2005040423
- 709 21. Chen S, Zhou Y, Chen Y, Gu J. fastp: an ultra-fast all-in-one FASTQ preprocessor. *Bioinformatics*.
710 2018;34(17):i884-i890. doi:10.1093/bioinformatics/bty560
- 711 22. Patro R, Duggal G, Love MI, Irizarry RA, Kingsford C. Salmon provides fast and bias-aware
712 quantification of transcript expression. *Nat Methods*. 2017;14(4):417-419.
713 doi:10.1038/nmeth.4197
- 714 23. Love MI, Sonesson C, Hickey PF, et al. Tximeta: Reference sequence checksums for provenance
715 identification in RNA-seq. *PLoS Comput Biol*. 2020;16(2):e1007664.
716 doi:10.1371/journal.pcbi.1007664
- 717 24. MATUMOTO M. A note on some points of calculation method of LD50 by Reed and Muench. *Jpn J*
718 *Exp Med*. 1949;20(2):175-179.
- 719 25. Nie J, Li Q, Wu J, et al. Quantification of SARS-CoV-2 neutralizing antibody by a pseudotyped
720 virus-based assay. *Nat Protoc*. 2020;15(11):3699-3715. doi:10.1038/s41596-020-0394-5
- 721 26. Ferrara F, Temperton N. Pseudotype Neutralization Assays: From Laboratory Bench to Data
722 Analysis. *Methods Protoc*. 2018;1(1). doi:10.3390/mps1010008
- 723 27. Pegu A, O'Connell SE, Schmidt SD, et al. Durability of mRNA-1273 vaccine-induced antibodies
724 against SARS-CoV-2 variants. *Science*. 2021;373(6561):1372-1377. doi:10.1126/science.abj4176
- 725 28. Li S, Roupheal N, Duraisingham S, et al. Molecular signatures of antibody responses derived from
726 a systems biology study of five human vaccines. *Nat Immunol*. 2014;15(2):195-204.
727 doi:10.1038/ni.2789
- 728 29. Braun RO, Brunner L, Wyler K, et al. System immunology-based identification of blood
729 transcriptional modules correlating to antibody responses in sheep. *NPJ Vaccines*. 2018;3:41.
730 doi:10.1038/s41541-018-0078-0
- 731 30. Anderson P, Nagler-Anderson C, O'Brien C, et al. A monoclonal antibody reactive with a 15-kDa
732 cytoplasmic granule-associated protein defines a subpopulation of CD8+ T lymphocytes. *J*
733 *Immunol*. 1990;144(2):574-582.
- 734 31. Labi V, Erlacher M, Kiessling S, et al. Loss of the BH3-only protein Bmf impairs B cell homeostasis
735 and accelerates gamma irradiation-induced thymic lymphoma development. *J Exp Med*.
736 2008;205(3):641-655. doi:10.1084/jem.20071658
- 737 32. Agur T, Ben-Dor N, Goldman S, et al. Antibody response to mRNA SARS-CoV-2 vaccine among
738 dialysis patients - a prospective cohort study. *Nephrology, dialysis, transplantation : official*
739 *publication of the European Dialysis and Transplant Association - European Renal Association*.
740 Published online April 2021. doi:10.1093/ndt/gfab155
- 741 33. Longlune N, Nogier MB, Miedougé M, et al. High immunogenicity of a messenger RNA-based
742 vaccine against SARS-CoV-2 in chronic dialysis patients. *Nephrology, dialysis, transplantation :*

- 743 *official publication of the European Dialysis and Transplant Association - European Renal*
744 *Association*. 2021;36(9):1704-1709. doi:10.1093/ndt/gfab193
- 745 34. Drakesmith H, Pasricha SR, Cabantchik I, et al. Vaccine efficacy and iron deficiency: an
746 intertwined pair? *Lancet Haematol*. 2021;8(9):e666-e669. doi:10.1016/S2352-3026(21)00201-5
- 747 35. Kernan KF, Carcillo JA. Hyperferritinemia and inflammation. *Int Immunol*. 2017;29(9):401-409.
748 doi:10.1093/intimm/dxx031
- 749 36. Teijaro JR, Farber DL. COVID-19 vaccines: modes of immune activation and future challenges. *Nat*
750 *Rev Immunol*. 2021;21(4):195-197. doi:10.1038/s41577-021-00526-x
- 751 37. Koc M, Toprak A, Arikan H, et al. Toll-like receptor expression in monocytes in patients with
752 chronic kidney disease and haemodialysis: relation with inflammation. *Nephrology, dialysis,*
753 *transplantation : official publication of the European Dialysis and Transplant Association -*
754 *European Renal Association*. 2011;26(3):955-963. doi:10.1093/ndt/gfq500
- 755 38. Nagai K. Dysfunction of natural killer cells in end-stage kidney disease on hemodialysis. *Ren*
756 *Replace Ther*. 2021;7(1):8. doi:10.1186/s41100-021-00324-0
- 757